ISSN 0280–5316
ISRN LUTFD2/TFRT--5623--SE

Analog and Digital Signal Processing in an Optical Application

Martin Almers

Department of Automatic Control
Lund Institute of Technology
August 1999

Department of Automatic Control
Lund Institute of Technology
Box 118
SE-221 00 Lund Sweden

Document name
MASTER THESIS

Date of issue
August 1999

Document Number
ISRN LUTFD2/TFRT--5623--SE

Author(s)
Martin Almers

Supervisor
Per Hagander
Anders Rosenqvist (Cellavision)

Sponsoring organisation

Title and subtitle

Analog and Digital Signal Processing in an Optical Application

Abstract

The thesis consists of two parts.

Registration of Digital Images

Registration of images is a fundamental task in image processing. This is to match two or more images taken, for example, at different times, from different sensors or from different points of view. The methods used to register images are striving for a similarity metric indicating when the images are correct registered. A similarity metric gives a measure of the degree of similarity between an image and a template. The approaches to find a good metric have been done looking at statistics in the images, e.g. correlation between them. A new similarity metric, the Focus Similarity Metric, invented by personnel at CellaVision AB is here being introduced. There are patents pending. Below it will be shown that it is a very robust algorithm.

It is a similarity metric based on a focus function, i.e. two added images are most aligned when they, together, are as focused as possible according to a focus function. Given some tuning, the images can be registered using the Focus Similarity Metric if they differ in scale or have been translated or rotated. They can even have been manipulated and noisy. The metric is also insensitive to intensity differences between the images and gives a very well defined maximum. Furthermore, it is fast and easy to implement.

Control of CD-pickup

A CD-pickup is used to focus for example a diode laser beam at a CD-record. The pickup is moved using magnetic coils. It has a small mass, which makes it very sensitive to external disturbances. In this application the problem is to control the position of the pickup insensitive to disturbances. In the thesis identification and analysis of the pickup is made. A controller is selected and realised with an analog circuit.

Key words

Classification system and/or index terms (if any)

Supplementary bibliographical information

ISSN and key title
0280–5316

ISBN

Language
English

Number of pages
50

Recipient's notes

Security classification

Analog and Digital Signal Processing in an Optical Application

Martin Almers
Dept. of Automatic Control, Lund University
P.O. Box 118, SE-221 00 Lund, Sweden
e-mail: martin.almers@cellavision.ideon.se

Supervisors: Anders Rosenqvist[1], Per Hagander[2]
Examiner: Per Hagander[2]

[1]Cellavision AB, Ideon Research Park, SE-223 70 Lund, Sweden
[2]Dept. of Automatic Control, Lund University, P.O. Box 118 SE-221 00 Lund , Sweden

Acknowledgements

First and foremost I would like to express my sincere gratitude to my supervisor Anders Rosenqvist, for his generous help.

I would also like to thank Per Hagander, Daniel Elvin, Lars Rydén, Anders Heyden, Erik Linderup, Mattias Mårtensson, Per Sennmalm, Björn Wallin, Johan Håkansson, Niklas Larsson and Michael Lantz.

Contents

Aligning dissimilar digital images

Control of CD-pickup

Registration of Digital Images

1. Overview

This thesis proposes a new similarity metric for registration of digital images.

There are a lot of medical applications for a similarity metric, e.g. for gamma ray images change detection purpose and alignment of digital X ray images. There is no restriction to the application of this method to the various other non-medical imaging techniques.

Images used for registration can differ in many ways. They can have been translated, scaled and rotated. The images can also be noisy, modified and there can be intensity differences between them (see figure 3a), 4a), 5a)).

In this thesis, the images have been grabbed in different colours at different instants using a microscope.

The computer comparison of two images requires a registration step, which is usually performed by optimising a similarity metric with respect to the registration parameters.

There exist metrics using different approaches to find a similarity metric that is able to make a correct registration of images, e.g. to look at correlation between the images [5] and Stochastic Similarity Measure [2] which is using noise in the images (see chapter 3).

In this thesis a new class of similarity metric is introduced. The metric is based on how focused the images are. It was invented by personnel at CellaVision AB. There are patents pending. Below the metric is being thoroughly examined.

Some basics of digital image processing are first given. Then existing similarity metrics together with the Focus Similarity Metric are described and compared.

2. Introduction to digital image processing

Digital image processing is a wide area. Below some basic concepts, used in later chapters, are explained.

How a digital image is represented is explained in 2.1. Translation, scaling and rotation of an image can be done with a transformation-matrix as shown in 2.2. Interpolation is discussed in 2.3.

More about basic concepts and methodologies for digital image processing can be read in [3].

2.1 Digital image representation

A digital image refers to a two-dimensional intensity function f(x,y), where x and y are integers and denote spatial coordinates. The value of f(x,y) at any point is proportional to the brightness of the image in that point. The image can be considered as a matrix whose rows and columns indices represent a point in the image, where the value in that point identifies the corresponding brightness level. The elements of such a digital matrix are called pixels. High values of the pixels are bright, low values dark. In a black and white 8-bit image 0 is black and 255 is white.

The axis convention used is shown in figure 1.

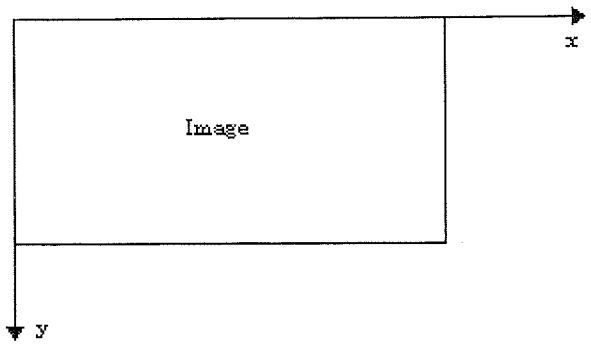

Figure 1. Axis convention for digital image representation

The intensities in the image may be grey levels or colour levels. A colour image usually consists of three single-coloured images, e.g. one blue, one red and one green image. However, there exist other representations (e.g. CYM).

2.2 Translation, rotation and scaling of a digital image

Translation of an image is to translate the pixel at point (x,y) to a new location by using coordinate displacements (T_x, T_y).

Rotation of an image is to rotate the pixels relative to a certain coordinate. The choice of the origin is important to get a good rotation. Having the middle pixel in an image as origin makes the rotation good. All the plots below are made using the middle pixel in the images as origin.

The matrix needed for translation, scaling and rotation is,

$$A = \begin{pmatrix} s \cdot \cos(\theta) & s \cdot \sin(\theta) & T_x \\ -s \cdot \sin(\theta) & s \cdot \cos(\theta) & T_y \end{pmatrix}$$

when the image is to be rotated with the angle θ, scaled by factor s and translated T_x, T_y pixels.

To map a pair of coordinates (x_1, y_1) of the first image to a new point (x_2,y_2), i.e. to transform a point in an image, just,

$$\begin{pmatrix} x_2 \\ y_2 \end{pmatrix} = A \cdot \begin{pmatrix} x_1 \\ y_1 \\ 1 \end{pmatrix}$$

This must be done for all points in the image to transform the whole image according to desired parameter values T_x, T_y, θ and s.

2.3 Interpolation

Interpolation is a way of estimating a signal at locations other than those where it was sampled (see figure 2). Images need two-dimensional interpolation, but since it is easier to illustrate one-dimensional interpolation, that is done here. Two-dimensional interpolation is based on the same concept.

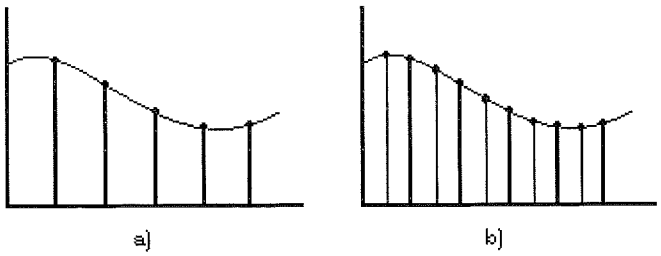

Figure 2. a). Original sampled signal, b) Original signal with interpolated values.

Interpolating new values can be done with many different functions. The interpolation function is a kind of weighting-function, i.e. it gives a value of how much a sampled point close to the interpolated is to be taken into consideration.

The interpolated value is calculated as

$$S'_{sample}(kt_{s2}) = \sum_{n=-\infty}^{\infty} S_{sample}(nt_{s1})\, r\,(kt_{s2} - nt_{s1}) \quad , \qquad \sum_{n=-\infty}^{\infty} r\,(nt_{s1}) = 1$$

where $r\,(k)$ is the interpolation function, S'_{sample} is the interpolated signal and S_{sample} is the original sampled signal.

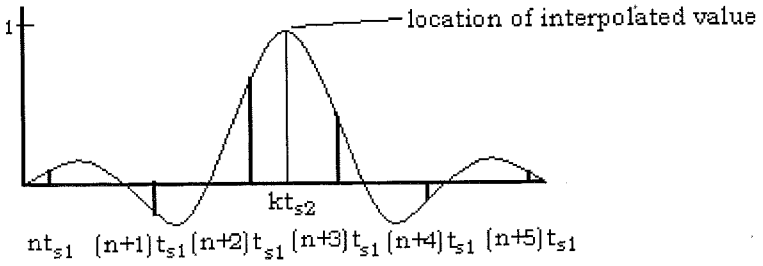

Figure 3. Interpolation function.

The ideal interpolation function is the sinc function (figure A4a)). All interpolation functions, except the ideal, affect the frequency content of the signal. The sinc function is not possible to realise because it is using points infinitely far away. It also has negative values that leads to the possibility that the interpolated value may be negative, which is a major drawback since intensities in an image can not be negative.

Many interpolation filters are windowed sinc functions, i.e. the values are zero outside a specific range. This gives realisability together with less complexity. But the windowing affects the frequency content in the images.

A common interpolation function used is the linear,

$$r\,(z) = 1 - |z| \qquad \text{when } |z| \le 1$$
$$= 0 \qquad \text{elsewhere}$$

The linear interpolation function is simple, easy to implement and fast to calculate.

The corresponding two dimensional function is called Bilinear (chapter 3.3.3).

The Parametric Cubic Spline is another common interpolation function,

$$
\begin{aligned}
r_{para}(z) &= (\alpha+2)|z|^3 - (\alpha+3)|z|^2 + 1 && \text{when } 0 \le |z| \le 1 \\
&= \alpha|z|^3 - 5\alpha|z|^2 + 8\alpha|z| - 4\alpha && \text{when } 1 \le |z| \le 2 \\
&= 0 && \text{elsewhere,}
\end{aligned}
$$

where α is a constant. With α=0.5 the central lobes approximates the sinc function.

The PCS is more alike the ideal than the linear, but it is more complex and not as fast to calculate as the linear. The PCS looks a lot like a windowed sinc function, but has almost no negative values (figure A6b)).

3. Similarity metrics

In order to measure the similarity between two images, some kind of measure is needed, a metric, a value that indicates if the images are fitting well together or not. A similarity metric gives a measure of the degree of similarity between an image and a template.

A general procedure to register two images (R(x,y) and G(x,y)) is:

1) One of the images is the reference, e.g. G(x,y). The other, R(x,y), is transformed, e.g. rotated, translated and scaled with, certain parameters. This gives $R_{trans}(x,y)$.

2) The similarity metric is calculated on the images G(x,y) and $R_{trans}(x,y)$.

3) The image R(x,y) is transformed with another transformation, i.e. the parameters are adjusted to get better registration. Then go to step 2) and repeat the procedure until the best transformation according to the metric is found.

There are different approaches to get a good metric. One way is to look at the correlation between the images, as briefly described in 3.1, another one is the Stochastic Sign Change Criteria (chapter 3.2).

The metric being proposed and studied in this thesis, the Focus Similarity Metric (FSM), is based on how focused the images are. It is shown to be very reliable. FSM is described and studied in 3.3.

In this thesis images of white bloodcells grabbed in green, G(x,y), and red, R(x,y), are used (figure A1a and A1b). They are used as an example of registration of images.

3.1 Correlation Metric (CM)

For a template T(x,y) and an image I(x,y), where T(x,y) is somewhat smaller compared to I(x,y), the two-dimensional normalised cross-correlation between them can be evaluated as,

$$C(u,v) = \frac{\sum_x \sum_y T(x,y) I(x-u, y-v)}{\sqrt{\sum_x \sum_y I^2(x-u, y-v)}}$$

C(u,v) gives a measure of the degree of similarity, the higher C(u,v) the better match. It must be normalised since local image intensity would otherwise influence the measure. By computing C(u,v) over different transformations it is possible to find the best match between the I(x,y) and T(x,y). If the images are noisy the maximum of the correlation may not be clear [5].

CM may not be able to register dissimilar and modified. Such images may lead to an incorrect registration.

More about CM see [5].

3.2 Stochastic Sign Change Criteria (SSC Criteria)

This method depends on the noise in the images.

Consider two images $I_1(x,y), I_2(x,y)$ where it is assumed that the images only differ because of the additive noise, which has zero mean. The noise variance may vary from one point to another. Let

$$S(x,y) = I_1(x,y) - I_2(x,y)$$

be the pixel-wise subtracted image. The S(x,y) values exhibit random fluctuations; those fluctuations are zero mean and with a variance which is the sum of the variances of the corresponding pixels of $I_1(x,y)$ and $I_2(x,y)$. Therefore the values of S(x,y) are positive or negative. Scanning S(x,y) line by line or column by column there are many sign changes among the scanned values. If $I_1(x,y)$ is transformed and the images are not well registered the mean of the number of positive and negative pixels of S(x,y) will no more be zero, there will be a reduced number of sign changes. It is this fact that the SSC uses. The SSC is defined as the number of sign changes in S(x,y), scanned line by line or column by column.

However, since this metric can not be used if the noise level is low compared with the precision of the digitisation, a variant of the SSC must be used then.

One variant to pass this problem is that a periodic pattern is added to one of the images.

$$I_1(x,y) = I_1(x,y) + q \qquad \text{if x+y is even}$$
$$I_1(x,y) = I_1(x,y) - q \qquad \text{if x+y is odd}$$

Then the same procedure as above is performed.

A drawback is that, since SSC can not be differentiated, derivative methods to find the best transformation can not be used.

SSC is nevertheless better than CM. SSC is less sensitive to noise and gives a more narrow and well defined maximum than CM.

See [2].

3.3 The Focus Similarity Metric (FSM)

All plots below were made using the images G(x,y) and R(x,y) (see figure A2a) and A2b). G(x,y) and R(x,y) are used as an example. The best alignment with G(x,y) and R(x,y) are achieved when the parameter values in translation, rotation and scaling are: T_x=1.2 pixels, T_y=0.8 pixels, s=1 and θ=-0.01rad.

The FSM is based on how focused the images are together. This means that the FSM uses a function that is meant to be used as a measure to see if an image is focused or not [4].

There are differences in the frequency domain between a matched and unmatched image. It is this fact that the FSM utilises (chapter 3.3.1).

Row by row and column by column the FSM is,

$$FSM = \sum_{y=0}^{N-1} \sum_{x=0}^{M-B-1} \left(\sum_{k=0}^{B-1} S(x+k, y) h(k) \right)^2 ,$$

where S(x,y) is an $[M \cdot N]$ sum image, h is a filter, a kind of band-pass filter,

$$h = \left[-1 \quad \underbrace{0 \ldots 0}_{n} \quad 2 \quad \underbrace{0 \ldots 0}_{n} \quad -1 \right] \qquad \text{and} \qquad B=2n+3.$$

In order to get a good metric, only the frequencies where the differences are clear should be amplified by h. Which frequencies that are being amplified using h depend of the value of n (chapter 3.3.1).

Registration of two images (R(x,y) and G(x,y)) with FSM is done like:

1) First the images are added, pixel by pixel. One of the images is the template, e.g. G(x,y). The other, $R(x,y,T_x,T_y,\theta,s)$, is transformed, $R_{trans}(x,y)$.

   $$S(x, y) = G(x, y) + R_{trans}(x, y)$$

2) The Focus Metric (FM) is calculated for the added image S(x,y).

   It is not necessary to calculate the FSM at every row and column. Calculating it infrequently does not have to give a worse result. The fewer rows and columns used, the faster the algorithm. Only columns could be used instead, or rows. More about this in 3.3.2.

3) The image, R(x,y), is then transformed with other parameters in the

transformation. Then step 1) is repeated. The procedure is repeated until the best transformation is found, i.e. the transformation when the FSM has the highest value.

Going through all the transformation possibilities can not be done. It is too time-consuming. This can however be done a lot faster (chapter 3.3.4).

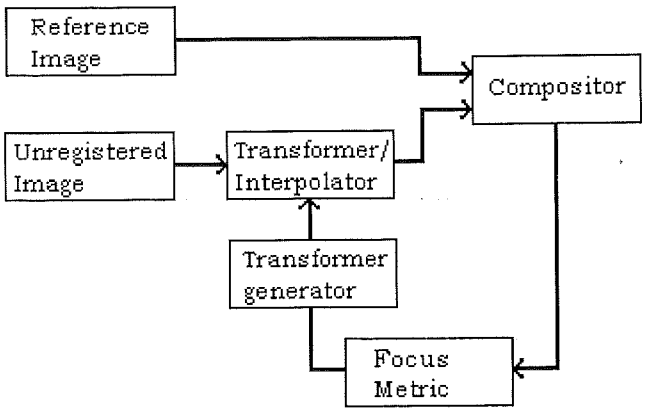

Figure 4. A block diagram of how registration with the Focus Similarity Metric works.

In order to be able to transform the image a proper interpolation must be used (chapter 3.3.3).

The value of the FSM indicates how registered the images are, the higher value the better matched. The value is not absolute, i.e. it only indicates that the images are more or less aligned.

The metric is shown to be very robust. When large disparities exist in the images the FSM still can find the correct registration. Registration of Modified green (figure A3)) and R(x,y) was correct. Misregistration does not occur even if noise is present or if there are intensity differences between the images, e.g. if different light sources were used when the images were taken (see figures A4 and A5).

3.3.1 The filter in the focus function

The filter in the FM is,

$$h = \left[-1 \quad \underbrace{0 \ldots 0}_{n} \quad 2 \quad \underbrace{0 \ldots 0}_{n} \quad -1 \right]$$

The number of zeros, n, used in the filter affects which frequencies that are being amplified and which frequencies that are being attenuated.

An image, g(x,y), can be filtered by convolution of the image and the filter,

$$i(x,y) = h(x) * g(x,y), \qquad \forall y$$

where i(x,y) is the filtered image and h is the filter.

Let the one-dimensional Fourier transforms of g(x,y), h(x), i(x,y) in the x-direction be G(u), H(u) and I(u). Then the convolution theorem [3] states that,

$$I(u) = G(u) \cdot H(u) \Leftrightarrow H(u) = \frac{I(u)}{G(u)}$$

This is used as a method of studying the filter in the frequency domain.

Three zeros, i.e. n=3, gives a filter like the one in figure 5a). n=10 gives a filter function amplifying a narrower spectrum (see figure 5b)). The more zeros used in the filter the narrower the spectrum being amplified is.

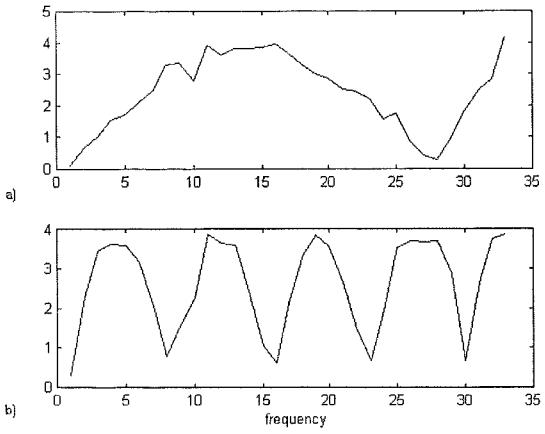

Figure 5. a) n=3, b) n=10.

If G(x,y) and R(x,y) are combined, the new image can be Fourier transformed. If the images are perfectly registered and the Fourier transform is calculated in the y-direction, it looks like figure 6a). The R(x,y) is then translated 2 and 4 pixels in the y direction, i.e. mismatched by 2 and 4 pixels. Figure 6b) and c) show the differences between the perfect registered images and the mismatched image Fourier transforms.

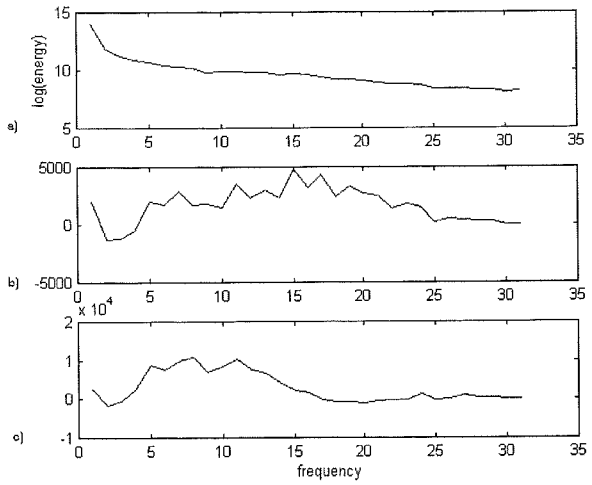

Figure 6. a) Fourier transform of perfectly registered images. b) and c) shows the difference between the frequency content in the perfectly registered and a mismatch in the y-direction by b) 2 pixels c) 4 pixels.

If the same images are being Fourier transformed in the x-direction, the transform looks like in figure 7. The difference is not as big in figures 7b) and c) that in figures 6b) and c). This shows that if the maximum for translation in y-direction shall be found, it is important that the FSM is calculated in the y-direction, i.e. rows. The corresponding effect occurs for translation in the x-direction.

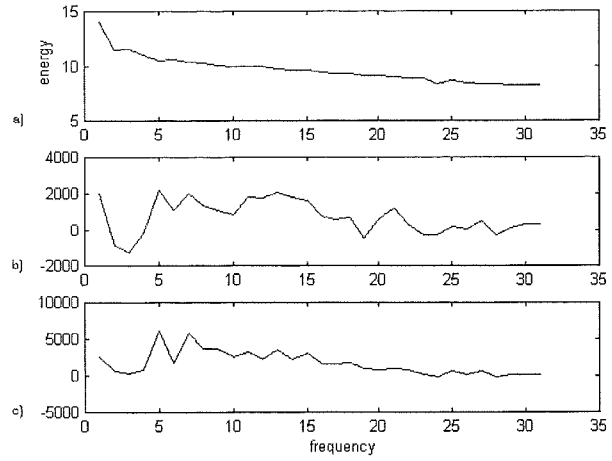

Figure 7. a) Fourier transform of perfect registered images. b) and c) shows the difference between the frequency content in the perfectly registered and a mismatch in the x-direction by b) 2 pixels c) 4 pixels.

The frequencies that differ between correct registered and incorrect registered images depend on the frequency content in the images. But the differences are close to the frequencies shown in figure 6 and 7.

This means that a filter should have about 3 zeros. The effect of having 2 or 4 zeros instead is not that big.

3.3.1.1 Using the filter

The FSM was calculated for G(x,y) and R(x,y), when R(x,y) was translated in the x and y directions. Parametric Cubic Bi-Spline interpolation was used.

The result with n=3 is shown in figure 8a). With n=10 it looked like in figure 8b). As can be seen the maximum is more narrow when n=3, but the surroundings close to maximum is not as smooth as when n=10. Using n=10 can be good when finding the maximum in a coarse search (chapter 3.3.4).

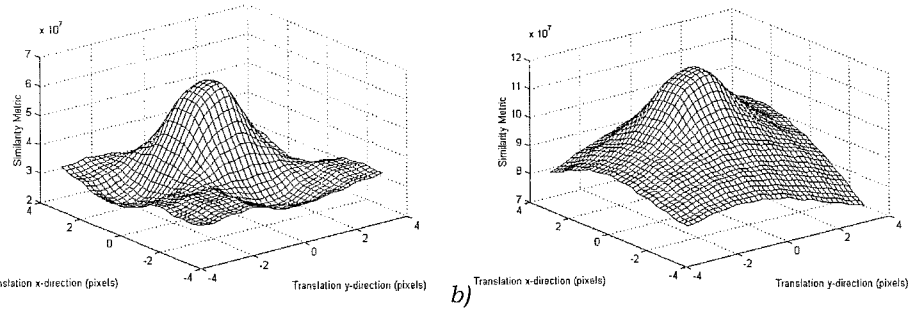

Figure 8. a) n=3, b) n=10.

3.3.2 Calculating the FSM

The more pixels used in the images when calculating the metric, the less noisy the metric is and the higher the probability is finding the correct registration. The reason is that using more pixels gives more information about the image. On the other hand, the fewer pixels used the faster the algorithm.

It is not necessary to calculate the metric at every row and column. There are different subsets of the image that can be used; a square, rows, columns or rows and columns, i.e. l_1. l_2, k_1 and k_2 do not have to be zero.

$$FSM = \sum_{y=l_1}^{N-1-l_2} \sum_{x=k_1}^{M-B-1-k_2} \left(\sum_{k=0}^{B-1} S(x+k, y)h(k) \right)^2$$

where $S(x, y)$ is a sum image.

Just using rows or columns would be the fastest solution. If only rows are used then the metric is not always reliable, i.e. if the images only contain horizontal lines, then the metric can hardly be used to register them. The corresponding is true for columns and vertical lines.

Using a square is reliable, if it covers an informative object in the images. Using a small square may miss all the important information in the images.

The rows and columns used do not have to be as wide and/or as high as the images themselves. The number of rows and columns that must be used and still give a good result, depend on the size of the images and the objects in the images.

In this thesis 80*80 pixel images were used. Using every second row and column in the metric gave almost the same result as using every row and column (figure A4a). Using every tenth was too sparse (figure A4b) to be able to align the images at a subpixel level. Every third row and column gave a very good result.

3.3.3 Interpolation methods

In this thesis two interpolation functions have been studied: the Bilinear and the Parametric Cubic Bi-Spline (PCBS) methods.

The Bilinear is interesting because of its simplicity. If it gives sufficient results, it is an obvious choice because it is very easy to implement and it is fast to calculate.

The PCBS is one of several possible cubic interpolation methods. Other cubic interpolation methods could have been used but they are all pretty alike. However, it is the general behaviour of the cubic methods that is important. The PCBS is a two-dimensional PCS.

A windowed sinc interpolation could also have been investigated, but it has as important drawback; the resulting values may be negative, and images intensities can not.

The Bilinear interpolation function is

$$r_{bi}(u,v) = (1-|u|)(1-|v|) \qquad \text{when} \quad |u| \le 1, |v| \le 1.$$
$$= 0 \qquad \text{elsewhere.}$$

The PCBS can be evaluated in two steps. First evaluation in one direction is done, as in chapter 2.3. This can be done either in the x- or y-direction.

$r_{pcs}(k)$ is then calculated in four rows or columns, giving $r_{pcs}(1)$, $r_{pcs}(2)$, $r_{pcs}(3)$ and $r_{pcs}(4)$. Then the interpolation is done in the same way as in the other direction, using the interpolated values from the first step.

Which direction of interpolation that is performed first, x or y, does not really matter since the resulting interpolation is almost exactly the same.

The PCBS is not as fast as the Bilinear, since the PCBS is more complex. It utilises a set of 16 pixels and the Bilinear interpolation utilises 4 pixels.

The frequency content in the image changes when interpolation with other methods than the ideal interpolator (the sinc interpolator) is used. Nevertheless, the Bilinear affects the frequency content in the image more than the PCBS does [7].

3.3.3.1 Using the PCBS and the Bilinear interpolations

Using the FSM for registration of images with the Bilinear or the PCBS clearly gives different results, as will be shown below.

Calculating FSM for the G(x,y) and R(x,y) for different translations in x and y directions with the Bilinear gives figure 9a). The green image has been the reference. Using the Bilinear interpolation does not give a smooth curve. In figure 9b) PCBS interpolation has been used instead. The PCBS gives a smooth curve with a well-defined maximum. This shows that it is easier to find the translation maximum with PCBS.

If the maximum is desired be found at a subpixel level, the PCBS or some other close related function must be used.

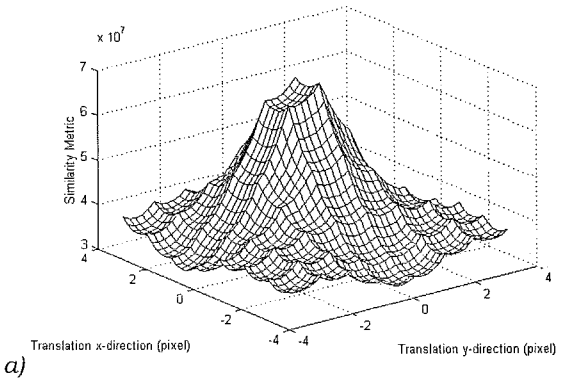

a)

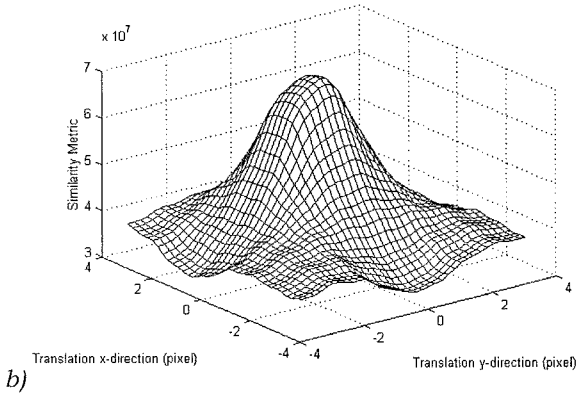

b)

Figure 9. T_x versus T_y a) Bilinear, b) PCBS.

The FSM gives values as shown in figure 10, when G(x,y) is reference and R(x,y) has been rotated and translated. In figure 10a) the Bilinear interpolation has been used. It gives a relatively smooth curve, where maximum can be found at a subpixel level. Figure 10 b) shows the result when PCBS is used. The PCBS gives a smooth curve.

Now the differences are not that big between the PCBS and the Bilinear interpolation functions. Both functions give a relatively smooth curve, yet the maximum is not as well defined with the Bilinear as with the PCBS.

Finding the rotation maximum at a subpixel level when the translation maximum is found does not need the PCBS interpolation, the simpler Bilinear is enough.

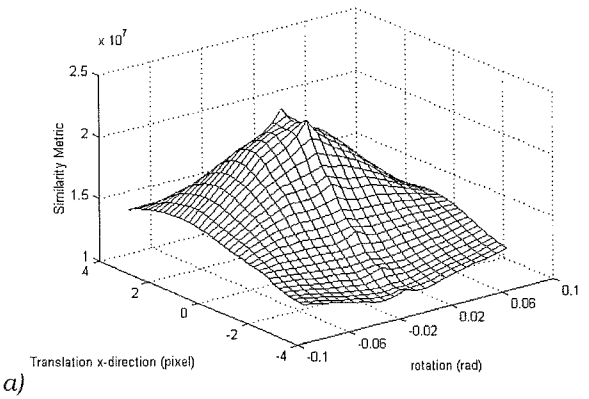

a)

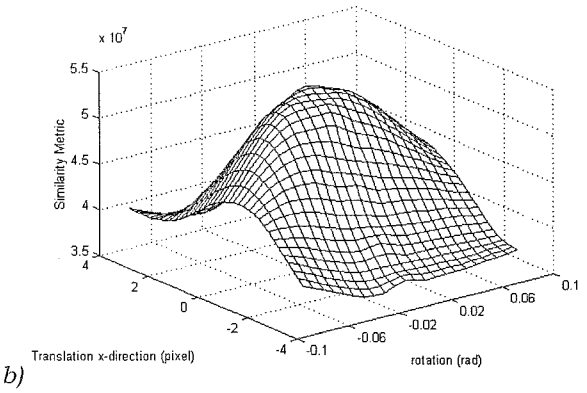

b)

Figure 10. Translation versus rotation, a) Bilinear, b) PCBS.

Under the same conditions as above figures 11a) and 11b) were made. Figure 11a) and 11b) show the FSM when the R(x,y) has been scaled and rotated using the Bilinear in a), and the PCBS in b).

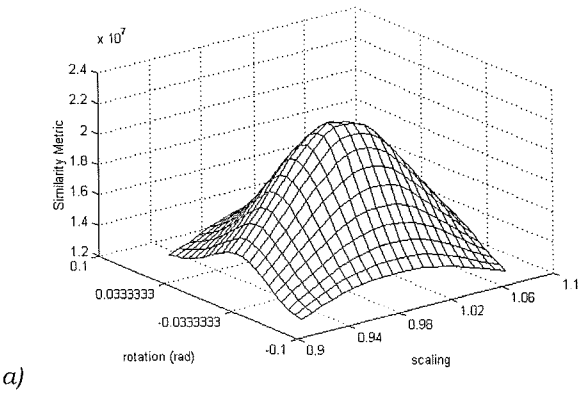

a)

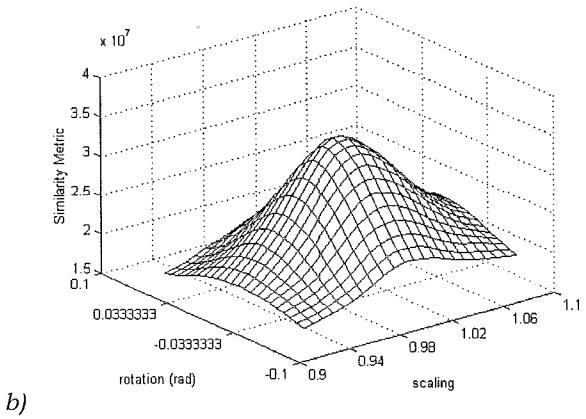

b)

Figure 11. Scaling versus Rotation, a) Bilinear, b) PCBS.

As can be seen the PCBS gives a smoother result in all cases. But it is more complex and therefore more time-consuming to compute.

In an implementation the choice of interpolation method will probably depend on the desired precision and time-demands.

3.3.4 Finding the maximum

Finding the maximum of a function, like the FSM, can be done in many ways. The most important thing when finding the fastest and the most reliable method is that the behaviour of the function should be well known. When the function has been carefully studied the method may be chosen.

The maximum of four parameters must be found in the transformation matrix used here: translation in x and y directions (T_x, T_y), scaling (s) and the rotation angle (θ).

The plots below were evaluated using the PCBS interpolation function and 3 zeros (n=3) in the focus filter.

Are T_x and T_y correlated? Having G(x,y) as reference and letting R(x,y) be translated gave an FSM like figure 12.

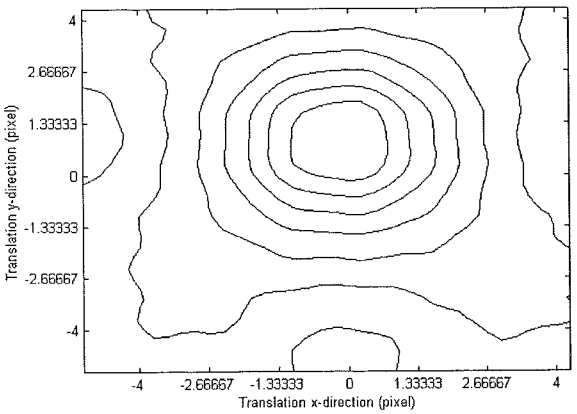

Figure 12. Translation in x-direction versus y-direction.

The parameters T_x and T_y are hardly correlated at all. That means that the T_x maximum can be found first and then T_y, or vice versa. The translation parameters can either be found both in the same two-dimensional optimisation or one at a time in two consecutive one-dimensional optimisations. The latter approach is simpler and probably quicker. To find the translation maxima the images can not be translated with more than 4 pixels.

With a good choice of coordinate representation, the optimisation with respect to the transformation parameters θ and s can be successfully made by consecutive optimisations in subspaces, i.e. not all parameters have to be varied in each optimisation. That saves time. One such good choice is to use the middle pixel as the origin of the image coordinates. This means that the interpolated image is then, in rotation and scaling, transformed around that middle pixel. The translation in x and y direction is not affected, but the correlation between changes in for example a translation parameter and the rotation or scaling parameter, are reduced.

The next effect studied was the correlation between T_x, T_y and s. G(x,y) was the reference and R(x,y) was scaled and translated in the x direction (see figure 13). Investigating T_y versus scaling is not necessary since T_x and T_y are more or less interchangeable.

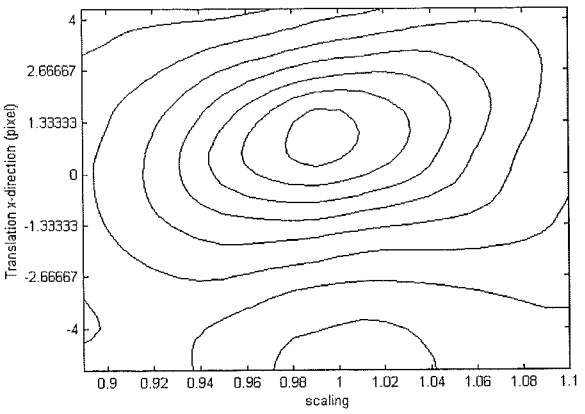

Figure 13. Translation versus scaling.

Experience from other images show that T_x and T_y the maxima can be found even if the images are having scaling differences with about 10%. The scaling maximum can be found if the images have been translated with about 2 pixels. This means that translation maximum should be found first, otherwise it is no use optimising the scaling parameter.

Figure 14 shows the correlation between translation and rotation. Translations T_x and T_y maxima can be found even if the images are rotated about each other with about 5 degrees. Other images show that they, in general, can be rotated about each other with about 5 degrees.

Finding rotation maximum when the images are translated with more than 2 pixel is difficult. This means that it is important that translation maximum is found first, otherwise it is no use finding rotation maximum.

Figure 14 was made under the same conditions as above.

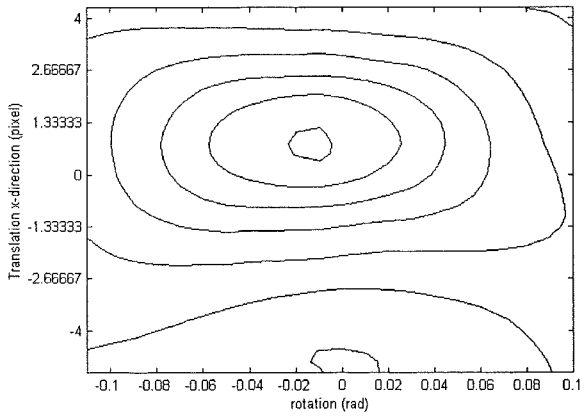

Figure 14. Translation versus rotation.

Figure 15, evaluated as above, shows that s and θ are not correlated if the parameters are not too far from the correct values.

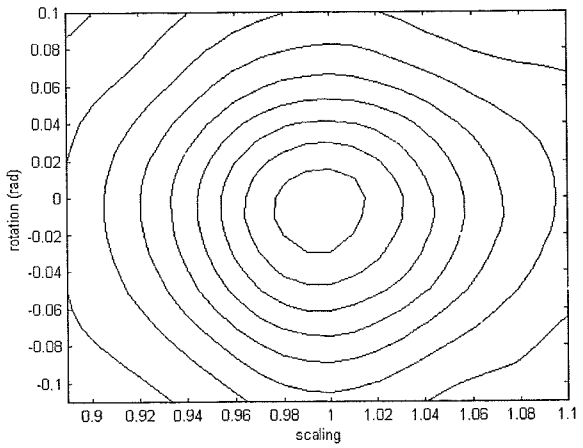

Figure 15. Scaling versus rotation.

Scaling differences can be as large as about 10% and the maximum of rotation can still be found. The rotation angle, θ, can be about 5 degrees and FSM still gives a distinct scaling maximum.

The images used are 80*80 pixels. Other sizes will give other results. With smaller images FSM will maybe not be able to find e.g. maximum in scaling with as large as 5 degrees, and with larger images maybe larger values than that can be handled.

If T_x, T_y, s and θ are not too far from the correct values the problem consists of four one-dimensional optimisations, i.e. the maxima of the parameters can be found one at a time.

To find the best transformation optimisation of the translation parameters should be done first, otherwise if the translation parameters are some pixels away from the correct ones, there is no meaning in trying to find the parameters for rotation and/or scaling.

As long as a coarse optimisation with respect to the translation parameters is done as a search with integer pixel steps, there is no need for interpolation. If subpixel accuracy is sought, interpolation of the transformed image has to be used. If there is a wish for derivative methods, interpolation has to be used in order to make the similarity metric differentiable with respect to the transformation parameters.

When knowing the translation parameters quite well, it is now meaningful to do an optimisation with respect to rotation and scaling. As

soon as at least one of these two parameters is involved in an optimisation, interpolation of the transformed image has to be used. The method of interpolation used will affect the achievable precision (chapter 3.3.3).

When coarse optimisation is done, 10 zeros could be used in the focus-filter. This makes it easier to find and get close to the maximum (see figure 8 b)). When fine optimisation is done 3 zeros should be used, it makes the maximum more narrow.

If the initial parameters are too far from the correct ones, the maxima still can be found, but not one-dimensionally. The parameters must then be optimised at least two at a time.

3.3.5 Different methods finding maximum

There are plenty of algorithms for optimisation to choose from. There are Ad-Hoc methods like the Simplex search and the Alternating variables [1].

Different derivative based line search methods, e.g. Steepest descent can be used.

Non-derivative methods like the Golden Section Search can also be used.

If the transformation parameter values are close to the correct ones, one-dimensional optimisation can be used. Optimisation in one dimension can be easily solved with one of the above mentioned methods.

Some of the interesting algorithms will be described below, and their pros and cons concerning the FSM function are discussed.

More about optimisation can be read in [1].

3.3.5.1 Golden section search

The Golden Section search works if the maximum is known to exist within a certain range. It is a non-derivative line search method.

First the function is evaluated at four points (see figure 16). There must be two points in the end of the range where the maximum exists. The other two points should be placed as in figure 16 with the ratio τ between.

$$\tau = \frac{1+\sqrt{5}}{2} \approx 1.618$$

Then the best point of the four is found. The two nearest points to the best point are kept. They are now the new outer points. If one of the outer points are the best the two nearest points to that is kept. New points are then evaluated as before between the new outer points. The best point among the new four points is determined and kept, and so on.

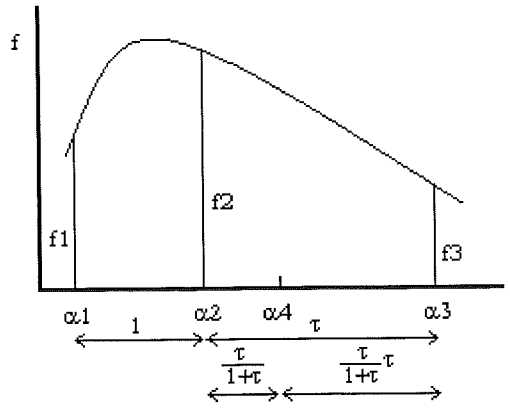

Figure 16. Golden section search.

This method is very reliable if it is known that the maximum exists within a certain range and the function is convex. The Golden section search is simple and implementation of the Golden section search is easy.

It is not as fast as the derivative methods can be but if reliability is important, then the Golden section search is a good choice.

The Golden section search works very well for the FSM function. If the parameter value is far from the correct one the FSM is not so smooth (figure A5), however the Golden section search works well for a function with a well-defined maximum and a surrounding that is not smooth. Derivative methods will have problems if that is the case.

3.3.5.2 Line search (derivative methods)

Here the basic principle of a derivative line search method is shown. There are a lot of ways solving the different steps.

The Line search starts by choosing any point x^0. Then repeatedly,

a) A direction of search S^k is determined.
b) A steplength α to maximise $f(x^k+\alpha S^k)$ is found with respect to x^k.
c) $x^{k+1}=x^k+\alpha^* S^k$

Different methods correspond to different ways of choosing S^k in a), based on the shape of the function. The problem in a) can be solved by using derivatives, e.g. like using the gradient in the Steepest Descent method. Using derivatives is risky when an exact derivative can not be calculated. With the FSM the derivatives can be calculated, but practically this is difficult. However the derivatives can be estimated, e.g. with forward differences,

$$f'(x) \approx \frac{f(x+h) - f(x)}{h}.$$

Step b) is carried out by repeatedly sampling the function and possibly its derivatives for different points x^k along the line. Steplength α that gives a significant approach towards optimisation must be found. Wrong choices of the steplength may lead to a reduction of $f(x^k)$. To approach optimisation $f(\alpha)$ must satisfy certain conditions, e.g. the Goldstein conditions,

$$f(\alpha) \leq f(0) + \alpha\rho f'(0)$$

and

$$f(\alpha) \geq f(0) + \alpha(1-\rho)f'(0)$$

where $\rho \in (0,1/2)$ is a fixed parameter.

Derivative methods are risky to use with the FSM. Far away from the correct parameter values, the function is not smooth. Using 10 zeros in the focus filter when coarse optimisation is done, will make it more reliable since the FSM will then be quite smooth, but even then the function may be to rough. The roughness makes it difficult to use derivative methods.

More about Line search methods can be read in [1].

3.3.5.3 Simplex search

The Simplex search is an Ad-Hoc method. The Simplex search in two dimensions is described below.

Three points in the shape of an equilateral triangle is placed in the surface, points 1, 2, 3 in figure 17. On the first iteration the vertex at which the function value is largest is determined, point 3 in figure 17. This vertex is then reflected in the centroid of the other vertices, forming a new simplex (points 2, 3 and 4 in figure 17). The function value at this new vertex is evaluated. The best value in the new triangle is determined. This is done until oscillation occurs, i.e. the maximum is close. Then the sides of the triangle are contracted to half length round the best point. The procedure is repeated until the precision desired is reached.

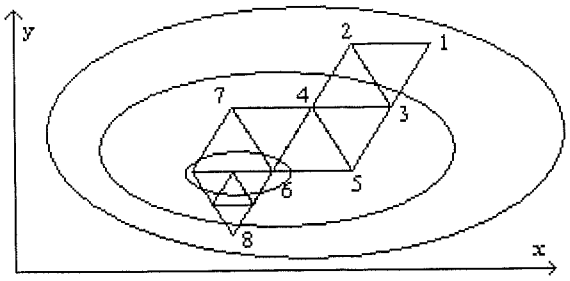

Figure 17. Simplex search.

3.3.5.4 Alternating variables

This is a simple method for optimisation in more dimensions than one.

Two variables, x and y, are both to be optimised. The alternating variable method starts at any point. Optimisation of one of the variables is done first, e.g. x. The other variable is kept fixed. After that the other variable is optimised, y, then x, then y and so on (see figure 18).

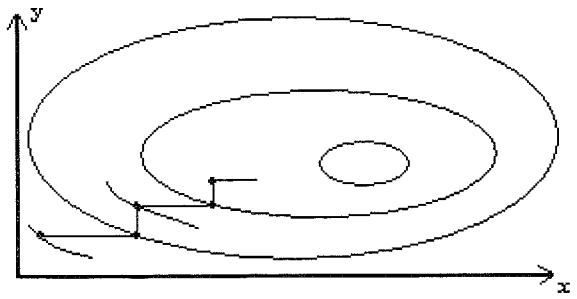

Figure 18. Alternating variables method.

The less correlated the variables, the fewer alternations are needed.
If more parameters are to be optimised, the same procedure as above is used.

Alternating variables is a simple method to implement but it is not the fastest and most reliable [1]. As can be seen in figures 13, 14 and 15 this method can be used at the FSM for optimisation in the different parameters.

4. Conclusions

A new class of similarity metric for digital images is proposed; the Focus Similarity Metric. The FSM differ from the classical ones mainly because it is not looking at statistics in the images. The FSM is based on how focused the images are together.

The new metric is shown to be very robust.

Control of CD-pickup

1. Introduction

A CD-pickup is used in a CD-player to focus a diode laser beam at a CD-record. The pickup can be moved up and down using magnetic coils, if a current is driven through the coils. When current is driven through the coils a force is exerted. The force is approximately proportional to the current. The direction of the current determines the direction of the force.

The pickup has a small mass. This makes it very sensitive to external disturbances. If someone pushes the table where the pickup is or walks in the room, there are large disturbances. The disturbances must be eliminated by active control.

The problem is to control the pickup to move vertically up and down in the z-direction, insensitively to disturbances.

In this application, it does not matter if there is a constant stationary error.

2. Laboratory equipment

The pickup consists of two parts. Two coils and an objective are attached to the same moving part of the pickup. By moving the coils, the lens moves. The other part consists of two stationary permanent magnets.

The coils and the objective are mounted to two plastic hinges, in the shape of a parallelogram. This makes the objective and the coils moving up and down vertically, z(t). If current is driven through the coils a force will be exerted and the pickup will move. The force is approximately proportional to the current. So the pickup will, ideally, be accelerated with the shape of the current i(t). Of course there is friction in the z-direction.

In order to be able to control the pickup a current i(t), an input to the actuator must be generated. A circuit like the one in figure 20 was used, where L is the inductance of the coils. This circuit makes the current through the load independent of the load impedance, assuming that the amplifier is ideal.

$$i(t) = \frac{V_{in}(t)}{R} \qquad (1)$$

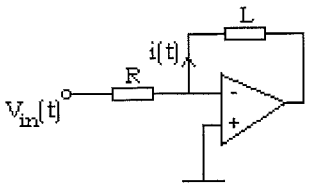

Figure 19. The electrical circuit. L represents the coils.

The operational amplifier is forcing i(t) to follow $V_{in}(t)$. $V_{in}(t)$ is then converted into a current through the coil which exerts a vertical force on the objective assembly.

To be able to measure the position of the pickup a slotted optical switch is used (figure 20). A slotted optical switch is a device that consists of a light emitting diode and a light detector. The light from the light emitting diode is infrared. The detector is a phototransistor that produces different currents depending on the intensity of the incoming infrared light.

A small extension is added to the pickup. The extension shields the light from the diode more or less depending on the position. The more the extension shields the light, the less current $i_{out}(t)$ from the detector. The slotted optical switch is linear in the area where the extension is covering the light. $i_{out}(t)$ is then a linear function of the position.

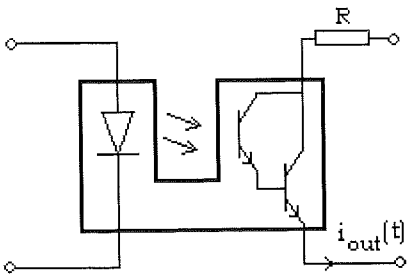

Figure 20. The slotted optical switch.

The system of pickup and slotted optical switch can be modelled by a block diagram like the one in figure 22.

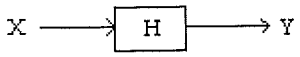

Figure 21. The block diagram of the system of pickup and slotted optical switch.

where X is the driving current, Y is the signal from the slotted optical switch and H is the system transfer function.

3. Measurements (identification)

The coils and the objective are a moving mass M. The coils can exert a force on the mass, which is also affected by other forces from the permanent magnet arrangement and the plastic hinges which have a damping effect. Therefore the pickup can ideally be represented as a spring-mass-damper system [8].

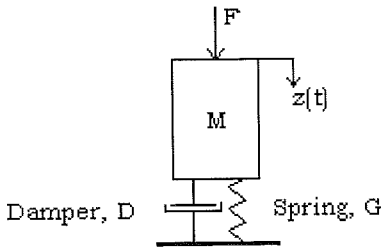

Figure 22. Spring-mass-damper system.

Figure 23 shows a schematic diagram of the principle parts with mass M, spring constant G and damping D, driven by a coil force F. The equation of motion of the mass is given by

$$M\ddot{z}(t) + D\dot{z}(t) + Gz(t) = F(t). \tag{2}$$

Using the LaPlace transform results in

$$MZ(s)s^2 + DZ(s)s + GZ(s) = F(s) \Leftrightarrow Z(s)(Ms^2 + Ds + G) = F(s) \tag{3}$$

The transfer function is then

$$H(s) = \frac{Z(s)}{F(S)} = \left(Ms^2 + Ds + G\right)^{-1} = \frac{1}{G}\left(\frac{Ms^2}{G} + \frac{Ds}{G} + 1\right)^{-1} \tag{4}$$

According to [8] $\omega_0 = \frac{M}{G}$ and $\beta = \frac{D}{2M}$. ω_0 and β in (4) gives

$$H(s) = \frac{1}{G}\left(\frac{s^2}{\omega_0} + \frac{2\beta s}{\omega_0} + 1\right)^{-1} \tag{5}$$

where β is the damping constant.

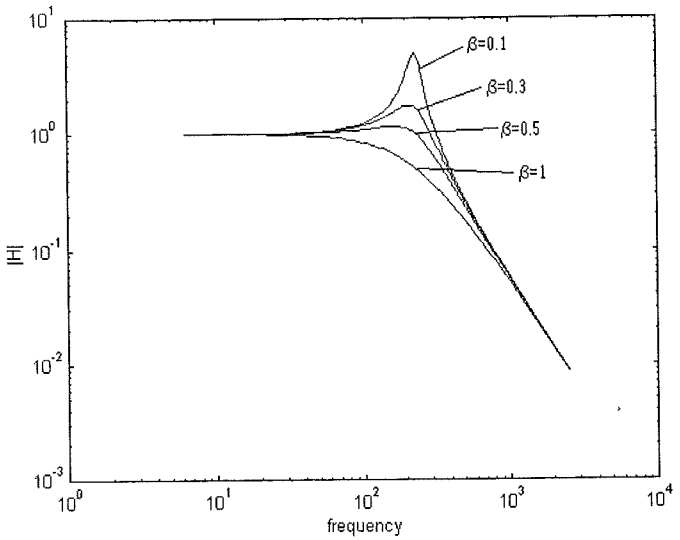

Figure 23. Amplitude Bode-plot of a spring-mass-damper system for different β.

Identification of the dynamic model can be done by determining the transfer function. An analysis of a Bode-plot can give the transfer function [6].

A Bode-plot consists of two plots; one amplitude and one phase shift plot.

By letting $V_{in}(t)$ be a sine, generated by a function generator, of different frequencies and measuring the voltage $V_{out}(t)$ and the phase shift, a Bode-plot for the system is made (figure 25). The measurements of $V_{out}(\omega)$, $V_{in}(\omega)$ and the phase shift are done for the open-loop system.

$$|H(\omega)| = \left| \frac{V_{in}(\omega)}{V_{out}(\omega)} \right| \qquad (6)$$

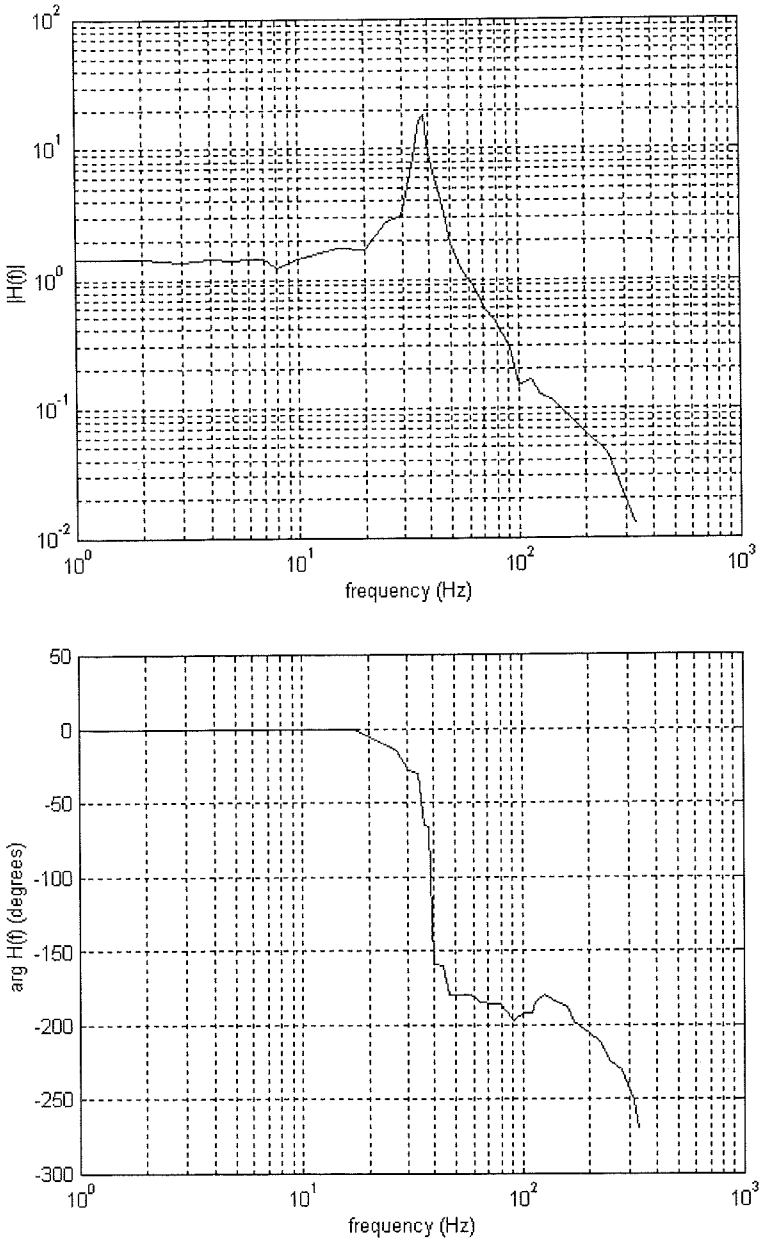

Figure 24. The measured Bode-plot.

4. Analysis

Figure 24 is compared to a spring-mass-damper system transfer function like in figure 23. At lower frequencies figure 23 and figure 24 looks the same, both figures having a resonance peak. At about 250 Hz the slope of the curve in the measured Bode-plot, figure 24, decreases. The measured Bode-plot has two resonance peaks. This is probably due to a parasitic resonance. The parasitic resonance may originate from too small stiffness between the objective and the coils.

The system with the parasitic resonance can be modelled as a spring-mass-damp system as in figure 25 [8].

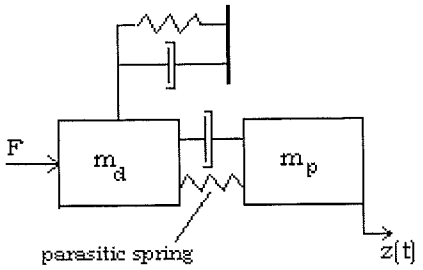

Figure 25. Mechanical model of the double spring-mass-damper system with a parasitic resonance.

The mass of the moving objective and driving magnet is m_p and m_d is the drive mass on which the driving force is exerted.

The transfer function for this system looks like

$$H(s) = \frac{k_5}{(k_1 s^2 + k_2 s + 1)(k_3 s^2 + k_4 s + 1)} \qquad (7)$$

After trying different parameter values the mathematical Bode-plot matched the measured very well (figure 26), with the constants $k_1 = \frac{1}{(37 \cdot 2\pi)^2}, k_2 = \frac{0.1}{37 \cdot 2\pi}, k_3 = \frac{1}{(250 \cdot 2\pi)^2}, k_4 = \frac{1}{250 \cdot 2\pi}, k_5 = 1.4$.

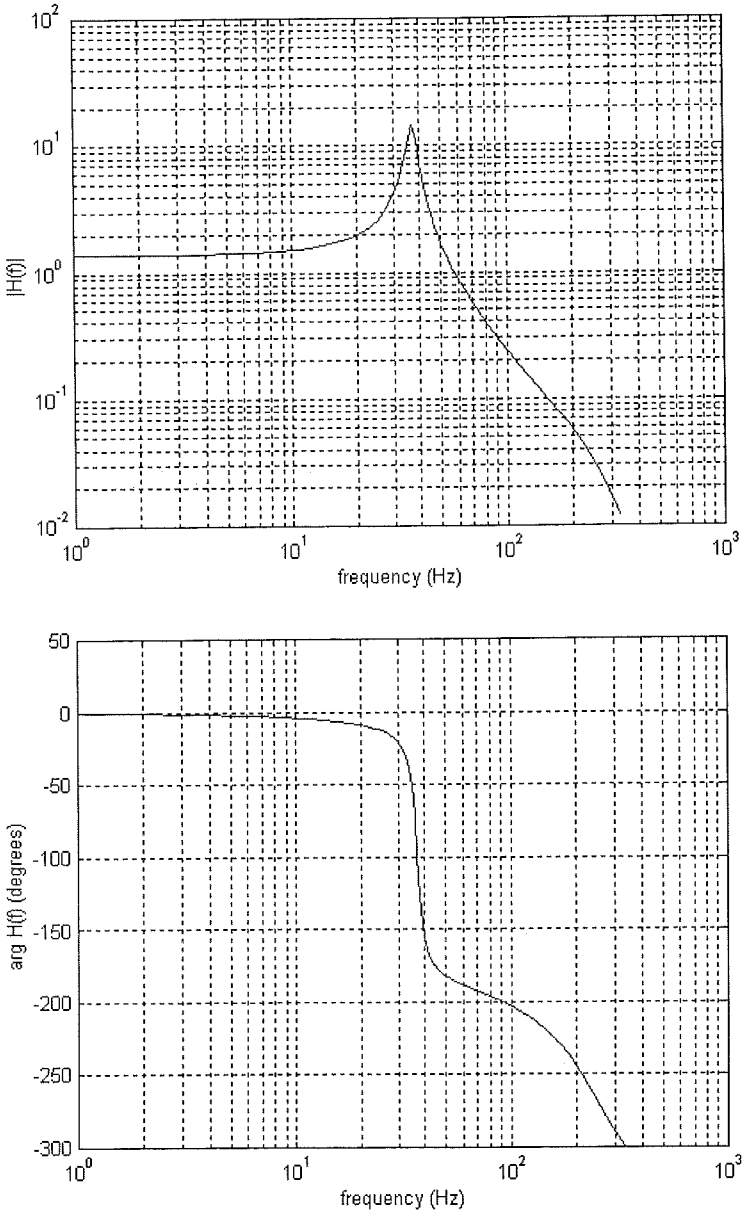

Figure 26. The Bode-plot of the modelled open-loop system.

One resonance peak is observed at about $\omega_1 = 37 \cdot 2\pi$ rad/s. The damping constant is β_1=0.05, identified in (7). The other resonance peak, the parasitic, is at $\omega_2 = 250 \cdot 2\pi$ rad/s. That resonance peak has almost no height. β_2=0.5 according to the transfer function (7).

5. Disturbances

At low frequencies of x(t) the measured output signal, y(t), looks like in figure 27.

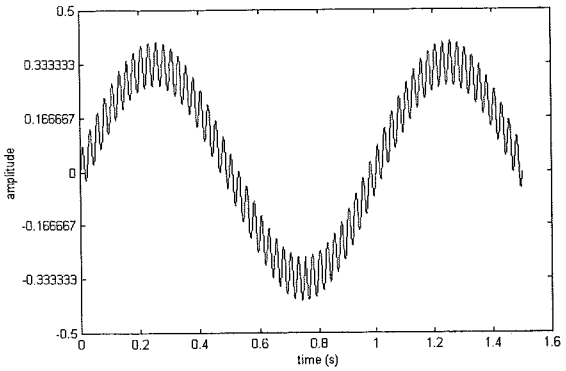

*Figure 27. y(t) at f=1 Hz. x(t)=sin(2*pi*f*t).*

These disturbances hardly exist at higher frequencies of x(t). The disturbances are probably caused by internal friction in the plastic hinges and have a frequency of about 40 Hz, which is close to the resonance frequency. The internal disturbances correspond to a movement in z-direction with amplitude of about 4 μm.

External disturbances such as touching the fundament where the pickup is mounted or footsteps on a wooden floor will cause accelerations within the pickup. Such accelerations introduce large changes in the pickup position, z(t). The external disturbances made the pickup move with frequencies around 40Hz.

As is shown below the external disturbances affect the system as an input to H in the same way as the current i(t).

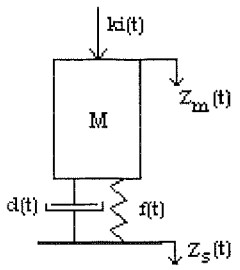

Figure 28. Model of the system. where $z_m(t)$ is the movement of the pickup , $z_s(t)$ is the movement of the fundament where the pickup is mounted.

The equation of acceleration of the pickup in the system in figure 28 is given by

$$\ddot{z}_m(t) = ki(t) - d(t) - f(t) \tag{8}$$

$$d(t) = k_d(\dot{z}_m(t) - \dot{z}_s(t)) \text{ and } f(t) = k_f(z_m(t) - z_s(t)), \tag{9}$$

where k_d is the damping constant of the damper and k_f is the spring constant. (8) and (9) gives

$$\ddot{z}_m(t) - \ddot{z}_s(t) = ki(t) - k_d(\dot{z}_m(t) - \dot{z}_s(t)) - k_f(z_m(t) - z_s(t)) - \ddot{z}_s(t) \tag{10}$$

The difference between the fundament and the pickup position is

$$z_{diff}(t) = z_m(t) - z_s(t). \tag{11}$$

Equations (10) and (11) result in

$$\ddot{z}_{diff}(t) = ki(t) - k_d\dot{z}_{diff}(t) - k_f z_{diff}(t) - \ddot{z}_s(t) \tag{12}$$

The relative position between the fundament and the pickup, $z_{diff}(t)$, is affected by $\ddot{z}_s(t)$ and i(t). If $ki(t) = \ddot{z}_s(t)$ then

$$\ddot{z}_{diff}(t) = -k_d\dot{z}_{diff}(t) - k_f z_{diff}(t) \tag{13}$$

This shows that i(t) can eliminate $\ddot{z}_s(t)$ and therefore that $\ddot{z}_s(t)$ affects the system as an input in the same way as the control signal i(t).

6. Simulation and selection of controller

Using feedback is a necessity to make the system less sensitive to disturbances and improve the systems ability to follow the input (figure 29).

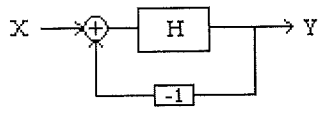

Figure 29. Closed-loop system.

The closed-loop system will have the transfer function

$$H_{cl}(s) = \frac{1}{1+H(s)}.$$

The system including the external disturbances, denoted N, is shown in figure 30.

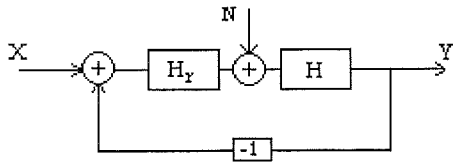

Figure 30. Block diagram of the closed system with external disturbances.

This gives, for the closed-loop system, including the controller $H_r(s)$,

$$Y(s) = \frac{H_r(s)H(s)}{1+H_r(s)H(s)}X(s) + \frac{H(s)}{1+H_r(s)H(s)}N(s). \qquad (14)$$

The goal is to design a controller that gives a system according to the specifications. The system should be insensitive to disturbances, while a stationary error in position is irrelevant.

A simple controller can consist of an amplification (P), an integration (I) and a derivative (D) part, or a combination of the different parts, e.g. a PD-controller.

By using an integrator the stationary error could be eliminated. Here, this is not a problem according to the specifications and therefore not necessary. The integrator would just slow the system down.

The pole-zero plot for the closed-loop system in figure 30, with H_r=1, looks like in figure 31.

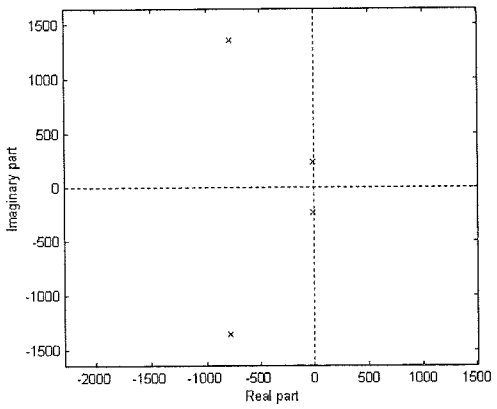

Figure 31. Pole-zero plot for the closed-loop system. The poles are represented with 'x'.

If the real part of the poles is positive, i.e. in the right half plane in a pole-zero plot, then the system is unstable [6]. Two of the poles in figure 32 are very close to the imaginary axis. These poles make the system sensitive. They should be moved away from the imaginary axis. The further away from the imaginary axis in to the left half plane the better the damping and the faster response.

The closer the poles are to the real axis, the less oscillation. If the poles are real then there is no oscillation at all.

Moving the poles that are close to the imaginary axis in to the left half plane can not be done with just a P-regulator. The poles can however be moved like that using a PD-regulator,

$$H_r(s) = K\left(1 + \frac{sT_d}{1 + \frac{sT_d}{N}}\right), \qquad N = 9 \tag{15}$$

where K is the amplification, T_d is the derivative time constant. An ideal PD-controller is here implemented using OP-amplifiers and analog circuits, this makes the PD-controller non-ideal. Such an implementation gives the denominator in (15). Having N=9 is reasonable in an analog implementation.

Using a PD-controller the system can be damped by placing the poles further away from the imaginary axis and therefore make the system less sensitive to disturbances, less oscillative and faster in response.

The root locus method shows how the poles in the transfer function vary with different amplification K [6]. If the open-loop transfer function is

$$H_s(s) = \frac{Q(s)}{P(s)} \tag{16}$$

then the root locus method is calculated as the roots of

$$P(s) + KQ(s) = 0 \tag{17}$$

Here the open-loop transfer function, $H_s(s)$, is (7) multiplied with (14),

$$H_s(s) = \frac{k_5 K\left(1 + sT_d/(1 + \frac{sT_d}{N})\right)}{(k_1 s^2 + k_2 s + 1)(k_3 s^2 + k_4 s + 1)}$$

Here, there should be as much damping as possible and still a maintained stability. This means that the poles should be as far away from the imaginary axis as possible.

By trying different T_d and plotting the root locus a good T_d and K can be found. For Td=0.005 the root locus looks like in figure 32.

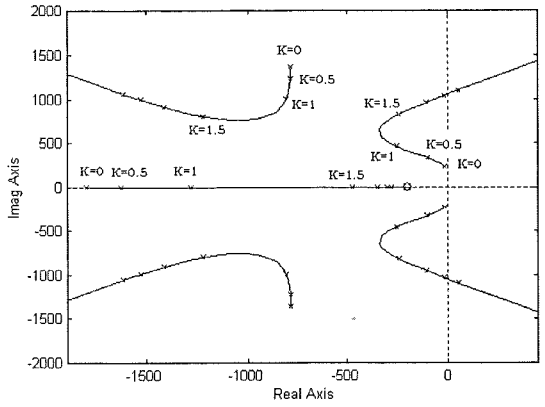

Figure 32.The root locus for T_d=0.005.

A T_d=0.005 is found to be good. Other T_d do not move the poles as far in to the left half plane as T_d=0.005.

A K=1.3 moves the poles are as far from the imaginary axis as possible (see figure 33). A K about 1.3 is a good choice.

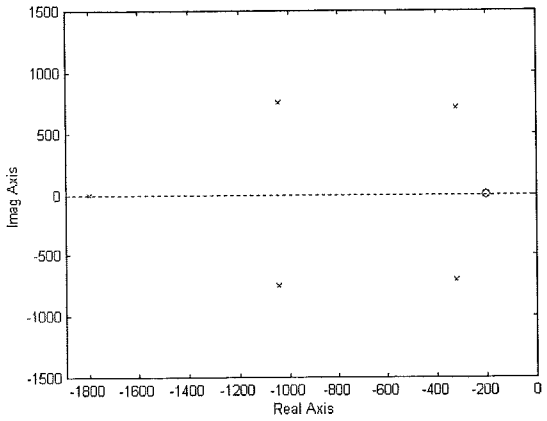

Figure 33. Pole-zero plot for the controlled system with T=0.005 and K=1.3. The poles are represented with '+' and the zeros with 'o'.

If K=1.3 and T_d=0.005 the impulse response for the controlled system looks like in figure 34.

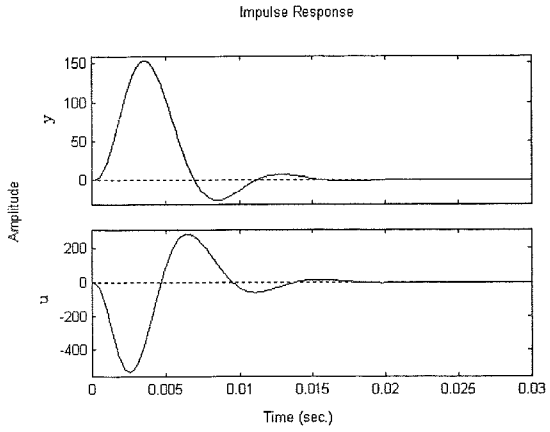

Figure 34. y is the impulse response and u is the control signal for the controlled system with T_d=0.005 and K=1.3.

7. Realisation

A PD-regulator can be built with a few electronical components. The whole system looks like in figure 35.

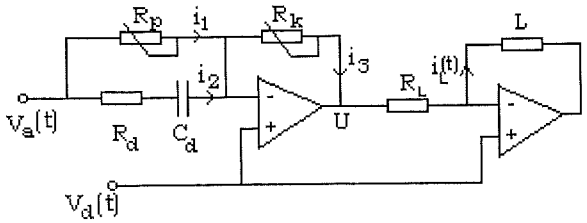

Figure 35. Electric circuit of the regulator and the pickup. V_d is the desired signal and V_a is the actual signal from the slotted optical switch.

The current through the load, the pickup, is

$$I_L(\omega) = \frac{U(\omega) - V_d(\omega)}{R_L} \tag{18}$$

$$I_3(\omega) = I_1(\omega) + I_2(\omega) \tag{19}$$

$$I_3(\omega) = \frac{V_d(\omega) - U(\omega)}{R_k} \tag{20}$$

$$I_2(\omega) = \frac{V_a(\omega) - V_d(\omega)}{R_D + \frac{1}{j\omega C_D}} \qquad \text{and} \qquad I_1(\omega) = \frac{V_a(\omega) - V_d(\omega)}{R_p} \tag{21}$$

Equation (19) and (21) give

$$I_3(\omega) = \underbrace{(V_a(\omega) - V_d(\omega))}_{-e}\left(\frac{1}{R_p} + \frac{1}{R_D + \frac{1}{j\omega C_D}}\right), \tag{22}$$

where e is the error. Combining (20) and (22)

$$V_d(\omega) - U(\omega) = -eR_k\left(\frac{1}{1 + j\omega C_D R_D} + \frac{1}{R_P}\right) \tag{23}$$

and then (18) and (23)

$$I_L(\omega) = \frac{e}{R_L}\left(\frac{j\omega C_D R_K}{1 + j\omega C_D R_D} + \frac{R_K}{R_p}\right). \tag{24}$$

If C_D and R_D are chosen so that $j\omega C_D R_D$ is small at low frequencies the approximation

$$I_L(\omega) = \frac{e}{R_L}\left(j\omega C_D R_K + \frac{R_K}{R_p}\right) \tag{25}$$

can be done. The circuit makes it possible to adjust K, T_d and N.

$$T_D = C_D R_p$$

$$K = \frac{R_K}{R_P}$$

$$N = \frac{R_p}{R_D}$$

The components in the circuit are not ideal. That is why R_k and R_p are potentiometers so that the resistances can be adjusted to get the right K and T_d.

8. Results

Adjustments of R_k and R_p resulted in a controller that damped the external disturbances well but not entirely. The disturbances affected the pickup too much for the controller to be able to eliminate them, the movements were too large.

One way to deal with the external disturbances is using an accelerometer. The external disturbances are accelerations that affects the system as an input to the transfer function H (see figure 30). If the accelerometer is connected as a subtracted input to H with carefully adjusted amplification K so that A is equal to the disturbances N, then the added external disturbances could be eliminated (figure 36).

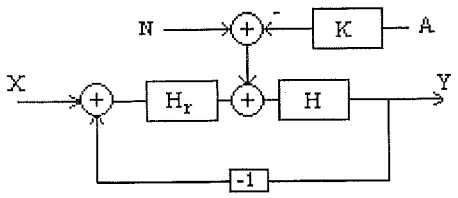

Figure 36. The system with an accelerometer. The accelerometer signal is denoted A and the external disturbance is denoted N.

At low frequencies, frequencies lower than 10 Hz, there are internal disturbances (see figure 28). These disturbances were not eliminated by the PD-controller. The internal disturbances may be caused by internal friction. These internal disturbances may be eliminated with another controller. A notch filter with a notch frequency at about 40 Hz may attenuate the internal disturbances.

The internal disturbances can maybe not be eliminated, it may be limitations in the mechanical system. The coils are maybe not able to move the pickup with control and stability with smaller movements than about 2 μm, the coils may be too small or the friction in the plastic hinges may be too large.

9. Appendix

The images used in the thesis are images of white blood-cells. They are grabbed in the colours green and red, G(x,y) and R(x,y).

At first they were 240*240 pixels. When they were used in this thesis they were downsampled to 80*80 pixels. The downsampling was made by

$$I_{downsample}(x,y) = \frac{1}{9}\sum_{k=0}^{2}\sum_{l=0}^{2} I(x+k, y+l)$$

where $I_{downsamle}(x,y)$ is the downsampled image and $I(x,y)$ is the original. This does almost not change the frequency content in the images at all (figure A1).

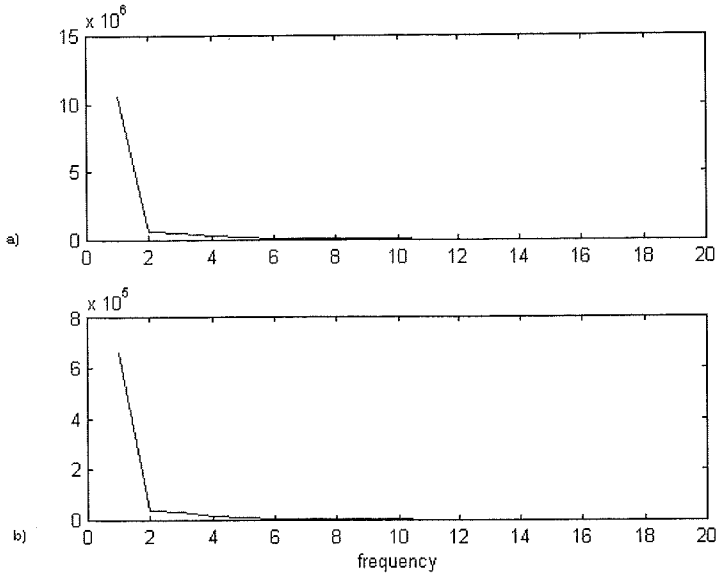

Figure A1 FFT of a) original image, b) downsampled image.

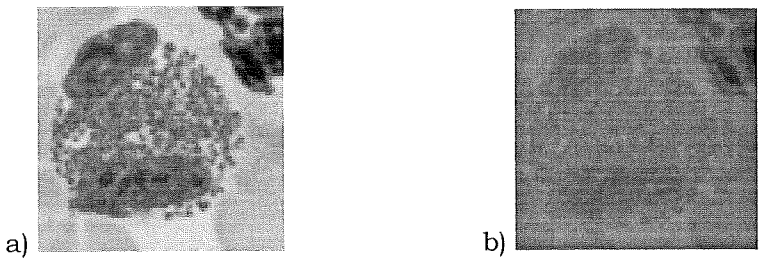

Figure A2. G(x,y) and R(x,y).

a)

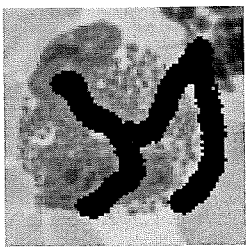

b)

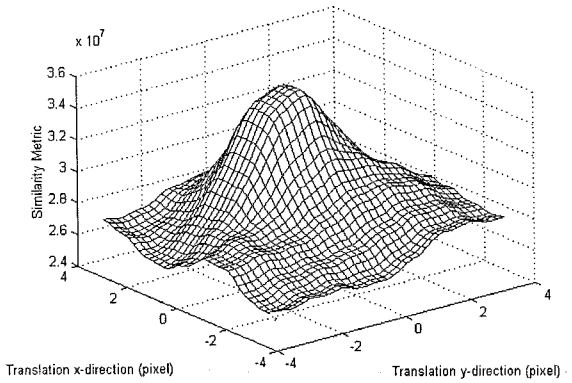

Figure A3.a) Modified G(x,y), b) Translation maximum.

a)

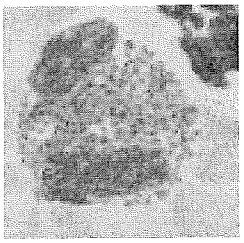

b)

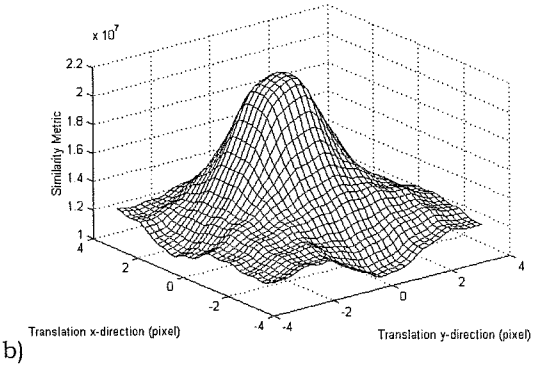

Figure A4. a) Noisy G(x,y), b) Translation maximum.

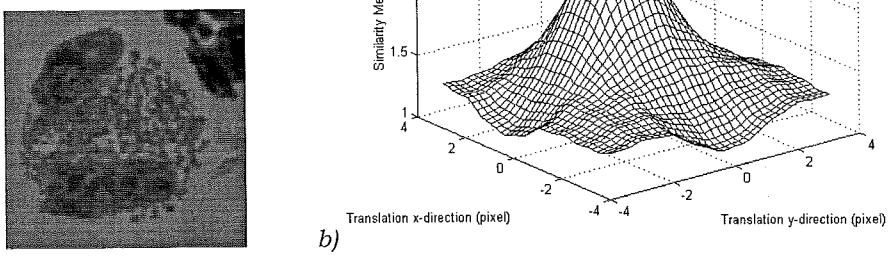

a) b)

Figure A5. a) Intensity R(x,y), b) Translation maximum.

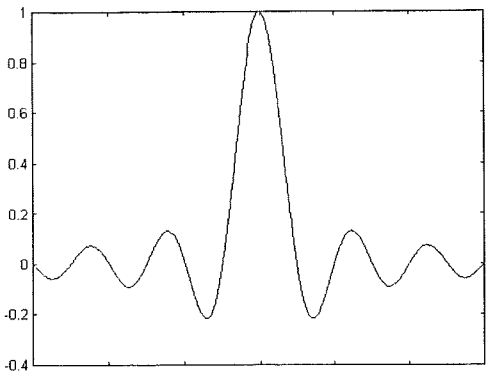

a)

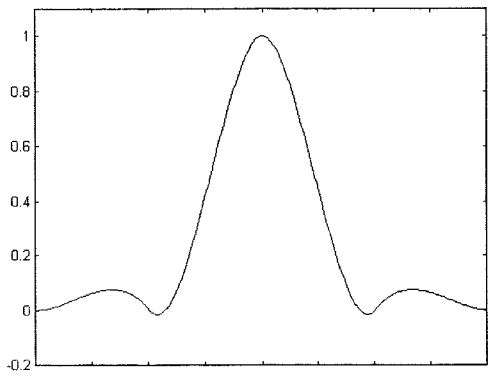

b)

Figure A6. a) Sinc function, b) PCS.

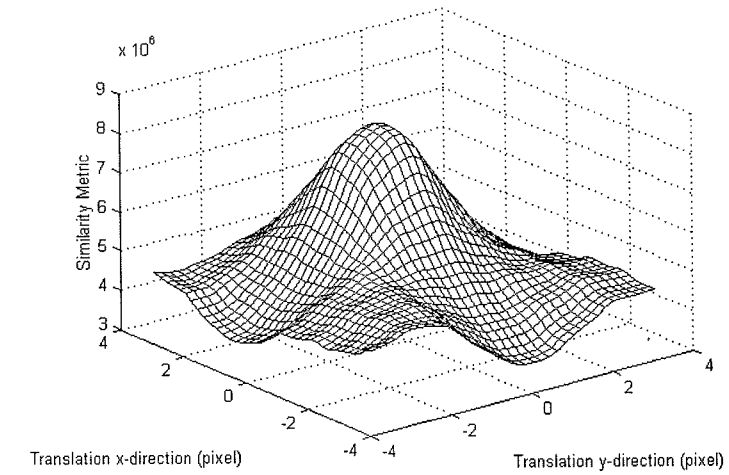

a)

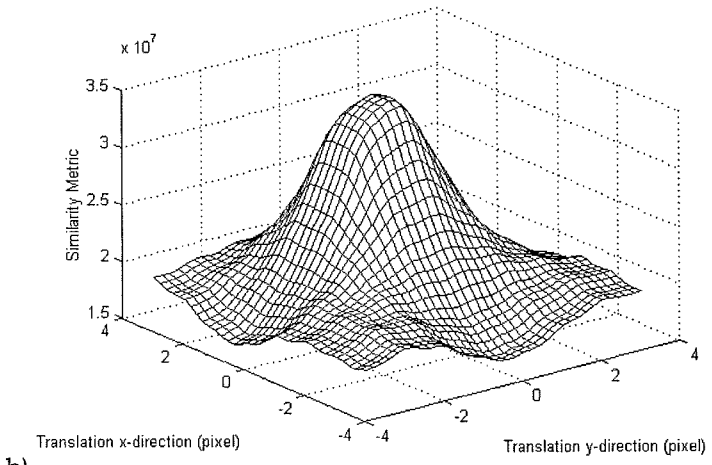

b)

Figure A7. a) Every tenth, b) every second column and row was calculated with the FSM.

10. References

[1] R. Fletcher , "Practical methods of optimization", John Wiley & Sons, second edition, 1987.

[2] A. Venot, J. F. Lebruchec, and J. C. Roucayrol, "A new class of similarity measures for robust image registration", 1984.

[3] R. C. Gonzalez and R. E. Woods, "Digital Image Processing", Addison-Wesley Publishing Company, Inc., 1993.

[4] M. Pettersson, " Autofocus and control of a hematology instrument", Master's thesis, Lund Institute of Technology, Department of Automatic Control, 1997.

[5] Lisa Gottesfeld Brown, "A survey of image registration techniques", ACM Computing Surveys, Vol. 24, No. 4, New York, 1992.

[6] Karl Johan Åström, "Reglerteori", Almqvist & Wiksell, second edition, 1985.

[7] Gerald C. Holst, "Sampling, aliasing and data fidelity", Spie Press, 1998.

[8] G. van Rosmalen et al, "Principles of optical disc systems", Bristol Hilger cop., chapter 4, 1985.